Electrical and structural properties of semi-insulating polycrystalline silicon thin films

S. Lombardo and S. U. Campisano
Dipartimento di Fisica della Università, Corso Italia, 57, I95129 Catania, Italy

F. Baroetto
Consorzio di Ricerca per la Microelettronica nel Mezzogiorno, Stradale Primosole, 50, I95100 Catania, Italy
(Received 4 May 1992)

Semi-insulating polycrystalline silicon layers with oxygen concentrations ranging from 2 up to 30 at. % O have been prepared by low-pressure chemical vapor deposition. After deposition, the samples were annealed at 920 °C for 30 min. Grain-size distributions, high- and low-frequency dielectric constants were measured, respectively, by transmission-electron microscopy, capacitance, and optical measurements as a function of the oxygen content. The average grain radius decreases with the oxygen content from 15 up to 2.5 nm. The current-voltage characteristics have been measured as a function of temperature in the range 80–450 K and under applied transverse electric fields up to $\approx 10^6$ V/cm. In weak-transverse-field conditions, the current density as a function of temperature shows two thermally activated regions at low and high temperatures, with activation energies of ≈ 0.14 and ≈ 0.54 eV, respectively. The application of transverse electric fields of the order of $\approx 10^6$ V/cm produces a current enhancement depending upon field intensity, temperature, and oxygen content. The results have been modeled by assuming thermionic emission, tunneling, and Frenkel generation in a long series of Schottky barriers formed at the boundary of the adjacent grains. The best-fit values of the model parameters indicate that for 30 at. % O a continuous SiO_2 shell, two monolayers thick, surrounds each grain. For lower oxygen contents this shell is discontinuous and the carrier transport parameters change considerably.

I. INTRODUCTION

Semi-insulating polycrystalline silicon (SIPOS) is an inhomogeneous material produced by chemical vapor deposition (CVD) of a mixture between SiH_4 and N_2O. The average film composition can be varied in a rather wide range of values by changing the flow ratio of the reacting gases. SIPOS is widely used as a passivating layer and a resistive field shield in high-voltage power devices;[1,2] the presence of free carriers within the passivation layer allows the screening of undesired charged contaminants. Conductivity depends on oxygen concentration and allows to keep the electric-field distribution undisturbed close to the junction termination thus optimizing device characteristics at high voltages.

Despite the increasing number of applications, both microstructure and conduction mechanisms are far from being well established. Different groups have characterized either the structure or the electrical properties of SIPOS. The structure of SIPOS has been investigated by transmission-electron microscopy,[3] optical spectroscopy,[4,5] and electron spectroscopy.[6] Two opposite pictures are drawn from these investigations: one describes SIPOS as a continuous mixture of crystalline and amorphous silicon containing small clusters of SiO_2.[7] The other picture describes SIPOS as small silicon grains completely surrounded by SiO_x.[8] It is expected that these two structures will lead to different transport properties.

The bulk electrical characterization has been made as a function of temperature[7,9,10] or in the presence of transverse electric fields.[11,12] These measurements lead to various models to describe conduction mechanisms: one assumes thermionic emission dominating the high-temperature conduction and electron tunneling dominating the low-temperature behavior.[9] Another model describes the transport as dominated by Frenkel generation[11,12] in the presence of transverse electric fields; in this case the transport at zero transverse field is not described and no correlation with the microstructure is given.

In this paper we report the results of a systematic investigation on the electrical and structural characterization of SIPOS in a wide range of oxygen concentrations. The measurements have been made on materials whose characteristics have been rendered reproducible by a post-deposition thermal treatment. The results are compared with model calculations where most of the parameters describing the electron transport are calculated *a priori*, based on structural considerations. The excellent agreement allows a strict relationship between structure and electrical conduction.

II. EXPERIMENT

⟨100⟩ oriented Si substrates (126 mm diameter, *n* type, 1–5 Ω cm) were used for the experiments. Some substrates were coated with a 1.3-μm-thick thermal oxide. SIPOS layers 0.8 μm thick were then deposited in a low-pressure CVD reactor at 620 °C at a pressure of 390 mTorr. The N_2O to SiH_4 gas flow ratio was varied from 2.5% to 28% in order to get layers with different oxygen content: nominal compositions were 2, 4, 8, 15, and 30 at. % O. After deposition, 30-min anneal at 920 °C in a dry oxygen ambient was used to stabilize material struc-

ture and properties. On samples with high oxygen content deposited directly on Si, Rutherford backscattering spectrometry (RBS) of 2-MeV ^{4}He ions confirmed that the oxygen content coincides within a few percent with the nominal values. Plan view SIPOS samples, prepared by mechanical thinning and backside chemical etch, were observed in a JEOL 2010 transmission electron microscope operating at 200 kV accelerating voltage. Low-frequency dielectric constants were determined by capacitance measurements in aluminum/SIPOS/SiO_2/Si capacitors. High-frequency dielectric constants of SIPOS films deposited on Si were determined from the infrared transmittance oscillations in the 1300–4000 cm^{-1} wavenumber range.

Aluminum contacts were defined photolithographically in an interdigitated structure. The gap width between the contacts and the overall length of each contact were 70 μm and 7.8 cm, respectively. Temperature was controlled by mounting the sample in a thermostatic stage, which was placed inside a vacuum chamber, using a minimum amount of thermal grease. Temperature could be varied between 80 and 450 K, with an accuracy of ± 1 K. Voltages up to 250 V were applied between the Al contacts. Substrate bias was varied between -270 and $+270$ V, corresponding to transverse electric fields of the order of 10^6 V/cm. Current measurements were performed, after a few minutes from voltage applications, to allow the current to reach a steady-state value. In any case, no steady-state current was detected along the circuit line for substrate polarization. High reproducibility of electrical characteristics has been found.

III. RESULTS

RBS was adopted to determine film composition for SIPOS samples with high oxygen content. In fact, the scattering cross section from oxygen nuclei is small compared to Si, so that it has been possible to obtain a good signal-to-noise ratio for samples of nominal composition 15 and 30 at. % O. The measured average oxygen concentration is 15 ± 2 and 27 ± 2 at. %. We thus assume that all the samples have a composition given by the nominal value.

Transmission-electron microscopy (TEM) of plan-view samples revealed a fine-grain poly-crystalline structure, as illustrated in Fig. 1 for the case of a 15 at. % O SIPOS layer. High-resolution TEM observations did not allow us to determine the exact topology of the sample, i.e., if SiO_2 is present in the form of small precipitates or as an interfacial layer among adjacent grains. We have measured the grain-size distribution for various compositions; these distributions are quite wide, particularly at low O contents. The average grain radius as a function of film composition is reported in Fig. 2. The average radius decreases with increasing oxygen content from 15 nm at 2 at. % O to 2.5 nm at 30 at. % O. The vertical bars represent the size-distribution width. Their length is equal to 2σ, where σ is the standard deviation of the size distribution.

In Table I the low-frequency dielectric constants, determined by capacitance measurements at various oxygen concentrations, are reported. The values are almost coincident with the pure silicon dielectric constant (≈ 11) for oxygen concentrations less than or equal to 8 at. %, and decrease up to ≈ 8.2 at 30 at. % O. These values are in good agreement with those predicted on the basis of a two-phase dielectric medium model.[14] Also shown are the measured values of high-frequency dielectric constants. At 2 and 4 at. % O the measurements were not possible since no clear oscillation was detected in the IR transmittance spectra. The measured high-frequency dielectric constants are smaller than the low-frequency values, in agreement with the fact that for pure SiO_2 the dielectric constant goes from 3.85 at low frequency to 2.56 at high frequency.[15]

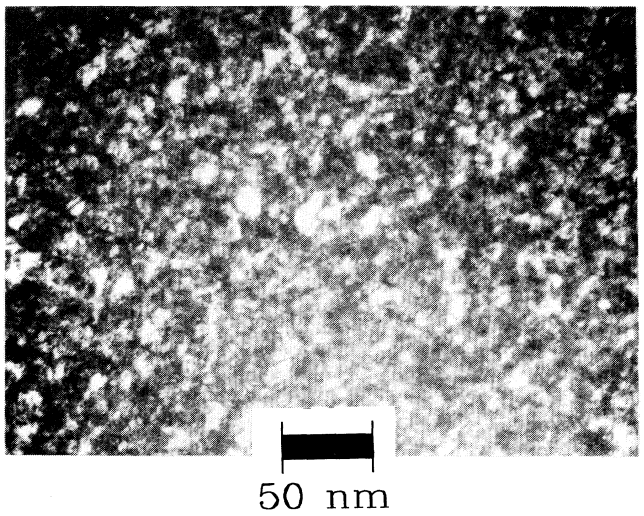

FIG. 1. Dark-field TEM plan-view micrograph of a SIPOS sample containing 15 at. % O. A fine-grain polycrystalline structure is evidenced by the micrograph.

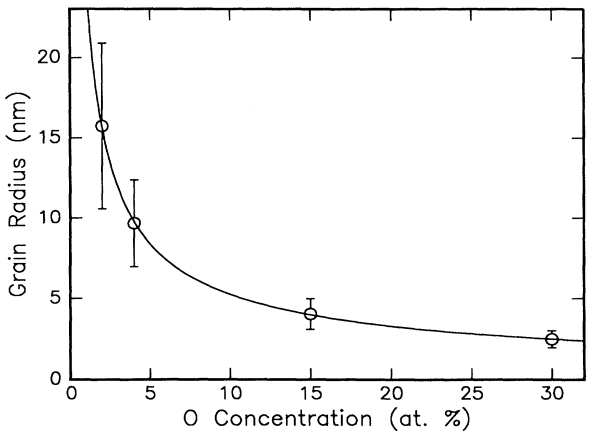

FIG. 2. Average grain radius measured by TEM as a function of film composition. The vertical bars represent the size distribution width. Their length is equal to 2σ, where σ is the standard deviation of the size distribution.

TABLE I. Low- and high-frequency dielectric constants measured as a function of the oxygen content.

at. % O	Low frequency	High frequency
2	11±2	
4	11±2	
8	10±2	7±1
15	9±1	8±1
30	8±1	5±1

The device structure used for the electrical characterization of the SIPOS layers is schematically drawn in Fig. 3 together with the bias and measurement circuit. The current density (J) measured at room temperature in samples containing 2, 8, and 30 at. % O is reported in Fig. 4 as a function of the voltage V applied between the Al contacts and for a substrate bias equal to 0 V. The $J-V$ characteristics are not ohmic, showing a complex dependence on the applied bias. The room-temperature resistivities are high, and for a 50-V bias the current densities range from $\approx 1\times 10^{-3}$ A/cm^2 at 2 at. % up $\approx 5\times 10^{-6}$ A/cm^2 at 30 at. % O.

The effects of intense transverse electric fields on the current densities measured at room temperature from materials containing 2, 8, and 30 at. % O are shown in Fig. 5. The two aluminum contacts are maintained at 0 and +120 V. For a substrate bias of −250 V the transverse electric fields range from $\approx 0.6\times 10^6$ V/cm at 2 at. % O up to 0.9×10^6 V/cm at 30 at. %, the difference being related to the different dielectric constants. In these conditions an increase of a factor ≈ 10 in current density is observed for materials containing up to 8 at. % O, while at 30 at. % O the increment is of a factor ≈ 1000. For positive substrate polarizations the current density appears quite insensitive to the substrate bias, in agreement with the data of Comizzoli and Opila.[11]

Figure 6 reports the current density as a function of temperature (T) for substrate biases (V_s) equal to 0, −180, and −250 V, for a sample containing 8 at. % O and with a 100 V polarization between the aluminum contacts. For a substrate polarization of 0 V, the $J-T$ characteristics (circles) show two activated regions, corresponding to activation energies of 0.53 eV at high temperatures and 0.14 eV at low temperatures, in good agreement with published data.[9] The different activation energies are due to two different conduction mechanisms operating at high and low temperatures, respectively. By biasing the substrate at −180 (triangles) or −250 V (crosses), the current density increases. The $J-T$ characteristics do not seem to follow a simple activated process, and the current density enhancement is negligible both at high and low temperatures. The enhancement

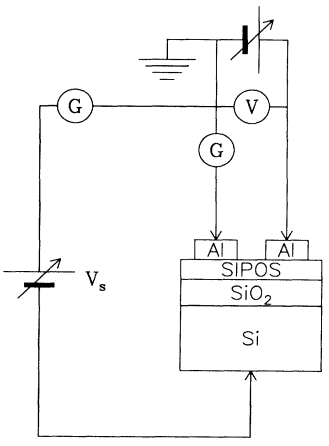

FIG. 3. Device structure used for the electrical characterization of the SIPOS layers drawn together with the bias and measurement circuit.

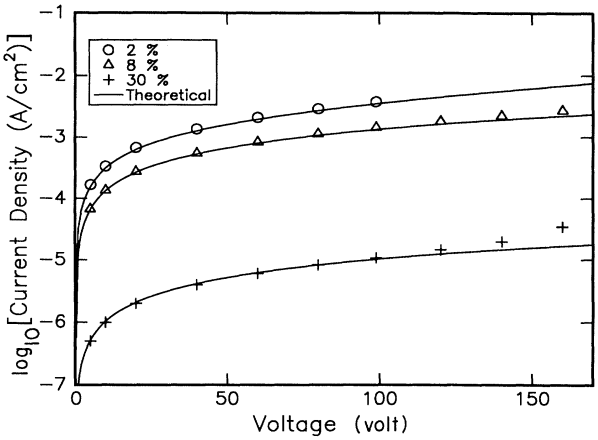

FIG. 4. Current density measured at room temperature in samples containing 2, 8, and 30 at. % O as a function of the voltage applied between the Al contacts and for a substrate bias equal to 0 V. The continuous lines are calculated by Eqs. (1) and (2).

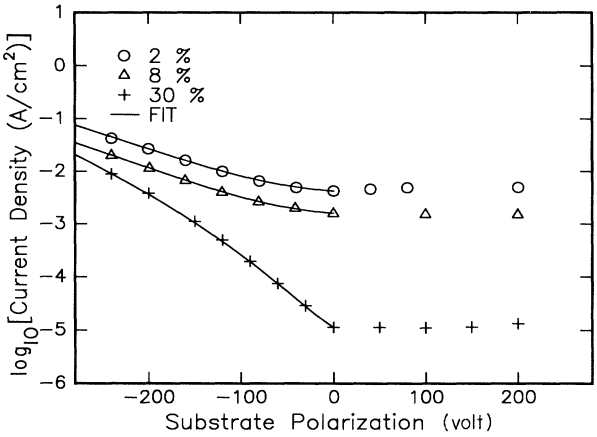

FIG. 5. Current density measured at room temperature in samples containing 2, 8, and 30 at. % O as a function of the substrate bias with the two aluminum contacts maintained at 0 and +120 V. The continuous lines are calculated by Eqs. (1), (5), and (6).

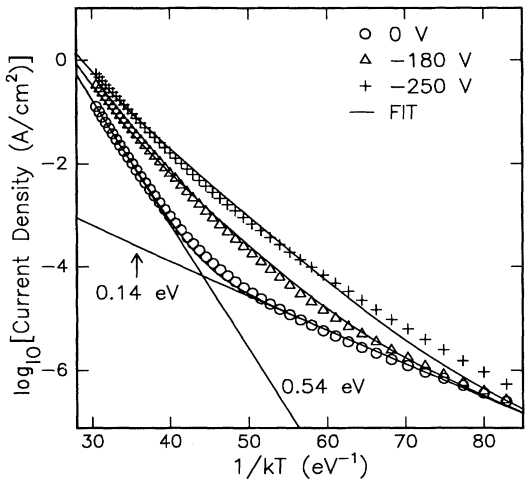

FIG. 6. Current density as a function of temperature for substrate biases equal to 0, −180, and −250 V, for a sample containing 8 at. % O and with a 100 V polarization between the aluminum contacts. The corresponding lines are the best-fit curves calculated by Eqs. (1)–(6).

is maximum in the temperature region in which the apparent activation energy of the $J-T$ curve at 0 V substrate bias changes from 0.53 to 0.14 eV. The same behavior has been observed for all the SIPOS films containing from 2 up to 15 at. % O.

A larger current density enhancement upon substrate bias has been found in the sample containing 30 at. % O, confirming the room-temperature data reported in Fig. 5. Figure 7 shows the $J-T$ characteristics for this material at 0 , −150, and −200 V substrate polarizations. At 0 V, the curve is similar to those for the lower oxygen contents, but the region characterized by a small value of activation energy is not visible because current densities were too low to be measured. These data show clearly the decrease with temperature of the current density enhancement due to negative substrate polarizations.

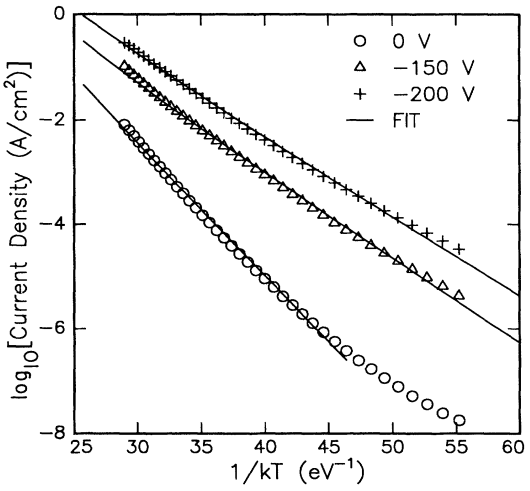

FIG. 7. Current density as a function of temperature for substrate biases equal to 0, −150, and −200 V, for a sample containing 30 at. % O and with a 100 V polarization between the aluminum contacts. The corresponding lines are the best-fit curves calculated by Eqs. (1)–(6).

IV. DISCUSSION

We have modeled the electrical characteristics of SIPOS taking into account grain size, dielectric constants, and their dependence upon the oxygen concentration. We have assumed that different conduction mechanisms dominate at different temperatures and depending on the transverse electric field. At high temperatures conduction is due to thermionic emission through barriers at the grain boundaries. Under large negative substrate polarizations the conductivity is enhanced by Frenkel generation.[13] At low temperatures conductivity is driven by tunneling of carriers through the barriers, and the Frenkel generation becomes negligible.

A. Unbiased substrates

The $J-T$ characteristics at $V_s=0$ V can be interpreted assuming the presence of a barrier for the free carriers motion at the grain boundaries. Tarng[9] has proposed that SIPOS conduction is due to free electrons emitted by oxygen shallow donor levels placed 0.16 eV below the conduction-band bottom edge.[16] Trapping of free electrons in deep acceptor states at the grain boundaries generates carrier depletion and midgap Fermi-level pinning near the grain boundary. The resulting band structure with symmetrical Schottky barriers at the grain boundaries is sketched in Fig. 8. According to this picture the barriers will drive the free carrier motion under external electric fields.

The current density J as a function of the voltage V between the aluminum contacts and the temperature T will behave as a long series of Schottky barriers. According to the models for conduction through Schottky barriers[17]

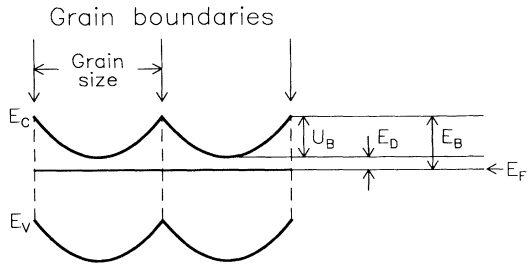

FIG. 8. SIPOS band structure with symmetrical Schottky barriers at the grain boundaries. E_C, E_V, and E_F are the edges of the conduction and valence bands and the Fermi energy, respectively. In the figure we report these energies as a function of the position respect to the grain boundaries. U_B is the electrostatic barrier caused by grain boundary charges and ionized O levels. E_B is the energy difference between the Fermi level and the conduction-band edge at the grain boundary. E_D is equal to E_B-U_B.

we have assumed

$$J=2J_s\sinh\left[\frac{qV}{2gk_BT}\right], \tag{1}$$

where q is the electron charge, k_B is the Boltzmann constant, and g is the ratio between the Al contacts gap length and the average grain diameter. J_s is a proportionality term depending on the conduction mechanism; in the high-temperature regime we assume thermionic emission above the barriers:

$$J_s=A^*f_pf_QT^2\exp\left[-\frac{E_B}{k_BT}\right], \tag{2}$$

where A^* is the Richardson-Fermi constant for electrons in silicon, equal to 260 $\mathrm{A\,cm^{-2}\,K^{-2}}$. E_B represents the Schottky barrier energy and is equal to the difference between the conduction-band bottom edge and the Fermi level at the grain boundary. E_B can be measured directly by the slope of the $J-T$ characteristics at high temperatures in an Arrhenius plot. We found E_B in the range 0.53–0.56 eV. The values confirm that the Fermi level at the grain boundary is pinned at midgap.

f_p and f_Q are factors taking into account the reduction in current density due to electron-phonon scattering and to quantum reflection at the barrier, respectively. f_p is approximately temperature independent and equal to ≈ 0.4.[17,9] We have assumed f_Q as a fit parameter whose value depends upon the oxygen concentration, considering that its value could dramatically depend on the presence of a thin oxide intergrain layer. Under this aspect, f_Q can be considered as a structural parameter that gives information about the grain boundary microstructure.

At low temperatures we assume that tunneling through the barriers dominates the conduction, thus

$$J_s=A^*f_{\mathrm{tun}}T^2\exp\left[-\frac{E_D}{k_BT}\right]. \tag{3}$$

f_{tun} represents the transmission coefficient for electron tunneling through the base of the barrier and E_D is the distance between the conduction-band bottom edge and the Fermi level in the undepleted grain center. Also in this case, E_D is measured directly by the slope of the $J-T$ curves at low temperatures. E_D spans the range 0.12–0.15 eV. The values are almost coincident with the ionization energy of the oxygen donor level previously indicated. Thus our measurements of E_B and E_D confirm fully the band structure sketched in Fig. 8.

The tunneling coefficient can be evaluated from the expression of Padovani and Stratton[18] slightly modified for this case of the *symmetrical* barrier. We have assumed

$$f_{\mathrm{tun}}=\exp\left[-\frac{2U_B}{\frac{qh}{4\pi}\left[\frac{N_D}{m^*\epsilon_{\mathrm{LF}}}\right]^{1/2}}\right], \tag{4}$$

where U_B is the barrier height, h is the Planck constant, N_D is the concentration of donor levels in the grain, m^* is the electron effective mass, and ϵ_{LF} is the low-frequency dielectric constant. We have assumed f_{tun} as fit parameter, since U_B and N_D can be only approximately obtained from the experimental data.

Least-squares fits of the experimental $J-T$ characteristics at $V_s=0$ V have been performed considering separately thermionic emission and tunneling through the Schottky barriers. The results of the fit procedures are reported as continuous lines on the corresponding experimental data in Figs. 6 and 7.

For oxygen concentrations from 2 to 15 at. % O, f_Q is constant and equal to 0.2. This value is in excellent agreement with that found in Au-Si Schottky barriers.[17] At 30 at. % O, f_Q becomes one order of magnitude smaller and is equal to 0.02. We attribute such sudden decrease to a transition in the SiO_2 phase microstructure from discontinuous to continuous shells, as proposed by Brunson *et al.*[19] If we assume that most of the oxygen present in SIPOS is segregated at grain boundaries in the SiO_2 phase, considering the average grain sizes, it results that for oxygen concentrations below 15 at. % O silicon grains are surrounded by SiO_2 shells approximately up to one monolayer thick. Probably these thin shells are discontinuous, and the silicon grains are partially in contact. On the other hand, at 30 at. % O we expect more continuous oxygen shells since their thickness is two monolayers. According to this picture, the sudden decrease of f_Q at 30 at. % O could be due to presence of this continuous oxide intergrain layer. In this case f_Q will become the transmission coefficient for electron tunneling through the oxide.

The best-fit values of f_{tun} are in the range $(6-23)\times10^{-10}$ going from 2 up to 8 at. % O. These values are in excellent agreement with those calculated with Eq. (4). In the equation, U_B can be evaluated from the difference E_B-E_D. N_D is then calculated by a simple electrostatic model[20] on the basis of the value of U_B. We obtain $U_B\approx 0.44$ eV and $N_D\approx 5\times10^{19}$ $\mathrm{cm^{-3}}$. Thus f_{tun} results $\approx 6\times10^{-10}$, in good agreement with the experimental values. Moreover, the increase of the transmission coefficient with the oxygen content can be interpreted on the basis of Eq. (4) as due to the slight decrease of the low-frequency dielectric constant going from 2 up to 8 at. % O.

The continuous lines in Figs. 4, 6, and 7 represent the best-fit curves calculated with the parameters indicated above. The agreement with the experimental data at $V_s=0$ V is good.

B. Biased substrates

We propose that the increase in drift current in the presence of transverse electric fields is due to Frenkel generation of free electrons from the acceptor deep level traps at the grain boundaries. Under intense transverse electric fields the binding energy of these trapped electrons, which is of the order of half silicon band gap, is substantially reduced. The reduction is given by

$$\Delta U=\left[\frac{q^3E_{\mathrm{el}}}{\pi\epsilon_{\mathrm{HF}}}\right]^{1/2}, \tag{5}$$

where E_{el} is the electric-field intensity and ϵ_{HF} is the high-frequency dielectric constant. E_{el} as a function of position can be calculated considering the potentials of the aluminum contacts and the substrate.

With a 100 V bias between the Al surface contacts and a -250 V substrate polarization, the electric-field intensities, dominated by the transverse component, are of the order of $\approx 1\times 10^6$ V/cm. The corresponding ΔU are of the order 0.3 eV. These values correspond to a substantial reduction in binding energy for the electrons trapped at the grain boundaries. Thermal excitations produce the emission of these light bound electrons on the top of the Schottky barriers. Their drift will not be affected by the Schottky barriers but will be influenced by the barrier quantum reflection and by the presence of thin oxide intergrain layers. Thus we have considered an additional term to J_s containing the contribution to current density due to free-electron Frenkel generation. The term is equal to the product of the occupied trap density at the grain boundaries (N_T) and the steady-state trap emissivity.[21] The resulting equation is

$$J_s = 54\frac{qm^* k_B^2 f_Q}{h^3} T^2 N_T \sigma \times \exp\left[-\frac{E_T}{k_B T}\right]\left\langle \exp\left[\frac{\Delta U}{k_B T}\right]\right\rangle , \quad (6)$$

where σ and E_T represent, respectively, the electron-capture cross section of the trap and its energy level referred to the conduction-band bottom edge. The presence of the transverse electric field reduces the trap binding energy, whose value becomes $E_T-\Delta U$. Consequently the generation current is increased by the factor $\exp(\Delta U/k_B T)$. We have to consider the average of this term, since the electric-field intensity depends on the position with respect to the aluminum contacts. This average has been approximated by considering only the two generation terms calculated in the SIPOS regions at the two contacts.

Least-squares fits of the J_T characteristics for negative substrate biases have been done considering the product $N_T\times\sigma$ and E_T as parameters. The continuous lines in Figs. 6 and 7 are the best-fit curves. According to our model, Frenkel generation becomes negligible at high temperatures since the term $\exp(\Delta U/k_B T)$ decreases with temperature. On the other hand, for sufficiently low temperatures the tunneling current prevails on the Frenkel generation.

The assumption of a single value for E_T is obviously a simplification of the problem. In fact, the comparison of calculated and experimental curves reported in Figs. 6 and 7 shows very good agreement at large current densities, i.e., at high temperatures, while at low current densities, i.e., at low temperatures, and for large transverse electric fields some deviation is observed in Fig. 6. This deviation may be due to the presence of tails in the trapping level distribution around E_T.

For all the oxygen concentrations we have obtained E_T in the range 0.55–0.62 eV. These values indicate that the trap levels are located at midgap. For oxygen concentrations in the range 2–15 % at., $N_T\times\sigma$ values resulted between 0.043 and 0.027. Here N_T and σ are expressed in units of 10^{13} cm^{-2} and 10^{-15} cm^2. At 30 at. % O, $N_T\times\sigma$ becomes $\approx$40 times larger, varying between 1.4 and 0.80. We attribute this increment to a large increase in the trap density in SIPOS with high oxygen content. This is reasonable, considering the variation in SIPOS microstructure is dependent on the oxygen concentration previously mentioned.

In Fig. 5 the continuous lines are best-fit curves calculated according to the model. The only fitting parameters were the dielectric constants and their values coincided well within the experimental errors with the measured values reported in Table I. At positive substrate bias the theoretical curves (not shown in this region) deviate significantly from the experimental data, overestimating the current densities. This behavior can be interpreted as due to the shielding of the electric field produced by free electrons attracted at the SIPOS/SiO_2 substrate interface.[11]

V. CONCLUSIONS

We have measured grain-size distribution, high- and low-frequency dielectric constants as a function of the oxygen content in SIPOS thin films. $J-T$ and $J-V$ characteristics under various substrate bias conditions have been determined in a large range of concentrations. The electrical measurements have been correlated to the data on grain size and dielectric constants by a model of electrical conduction. This model assumes that various conduction mechanisms are dominant at different temperature and substrate bias conditions. For small electric fields, thermionic emission and tunneling dominate at high and low temperatures, respectively. Large negative substrate biases, producing intense electric fields inside the SIPOS film, induce the emission of free electrons by Frenkel generation. This effect increases strongly the SIPOS conductivity. The fits of the experimental $J-T$ and $J-V$ characteristics suggest that the SIPOS microstructure changes at high oxygen contents. At low concentrations (2–15 at. % O), the SiO_2 phase volume fraction is not enough to insulate adjacent silicon grains. At 30 at. % O each silicon grain is surrounded by a two-monolayer-thick SiO_2 shell and the electrical properties change noticeably.

ACKNOWLEDGMENTS

We gratefully acknowledge Professor E. Rimini and Professor G. Ferla for many stimulating discussions. This work was partially supported by Progetto Finalizzato Materiali e Dispositivi per la Elettronica a Stato Solido, Consiglio Nazionale delle Ricerche.

[1]T. Matsushita, T. Aoki, T. Otsu, H. Yamoto, H. Ayashi, M. Okayama, and Y. Kawana, Jpn. J. Appl. Phys. Suppl. **15**, 35 (1976).
[2]T. Yamaguchi, K. L. Seaward, J. L. Sachitano, Jr., D. Ritchie, and S. Seto, IEEE J. Solid State Circuits **SC-13**, 472 (1978).
[3]J. Wong, D. A. Jefferson, T. G. Sparrow, J. M. Thomas, R. H. Milne, A. Howie, and E. F. Koch, Appl. Phys. Lett. **48**, 65 (1986).
[4]D. J. Olego and H. Baumgart, J. Appl. Phys. **63**, 2669 (1989).
[5]W. G. Andrä, G. Götz, H. Hobert, V. Misyuchenko, V. A. Samuilov, and V. Stelmakh, Phys. Status Solidi A **110**, 181 (1988).
[6]J. T. McGinn and A. M. Goodman, Appl. Phys. Lett. **34**, 601 (1979).
[7]M. Hamasaki, T. Adachi, S. Wakayama, and M. Kikuchi, Solid State Commun. **21**, 591 (1977).
[8]A. L. Nesbit, Appl. Phys. Lett. **48**, 38 (1985).
[9]M. L. Tarng, J. Appl. Phys. **49**, 4069 (1978).
[10]J. Ni and E. Arnold, Appl. Phys. Lett. **39**, 554 (1981).
[11]R. B. Comizzoli and R. L. Opila, J. Appl. Phys. **61**, 261 (1987).
[12]R. B. Comizzoli, H. T. Weston, Y. H. Wong, and J. E. Kohl, J. Electrochem. Soc. **133**, 1746 (1986).
[13]J. Frenkel, Phys. Rev. **54**, 647 (1938).
[14]D. A. G. Bruggeman, Ann. Phys. (Leipzig) **24**, 636 (1935).
[15]W. E. Beadle, J. C. C. Tsai, and R. D. Plummer, in *Quick Reference Manual for Silicon Integrated Circuit Technology,* edited by W. E. Beadle, J. C. C. Tsai, and R. D. Plummer (Wiley, New York, 1985), pp. 1–9.
[16]A. G. Milnes, *Deep Impurities in Semiconductors* (Wiley-Interscience, New York, 1973), p. 15.
[17]S. M. Sze, *Physics of Semiconductor Devices* (Wiley, New York, 1969).
[18]F. A. Padovani and R. Stratton, Solid State Electron. **9**, 695 (1969).
[19]K. M. Brunson, D. Sands, C. B. Thomas, C. Jeynes, and J. F. Watts, Philos. Mag. B **61**, 361 (1990).
[20]J. Seto, J. Appl. Phys. **46**, 5247 (1975).
[21]R. S. Muller and T. I. Kamins, *Device Electronics for Integrated Circuits* (Wiley, New York, 1986).

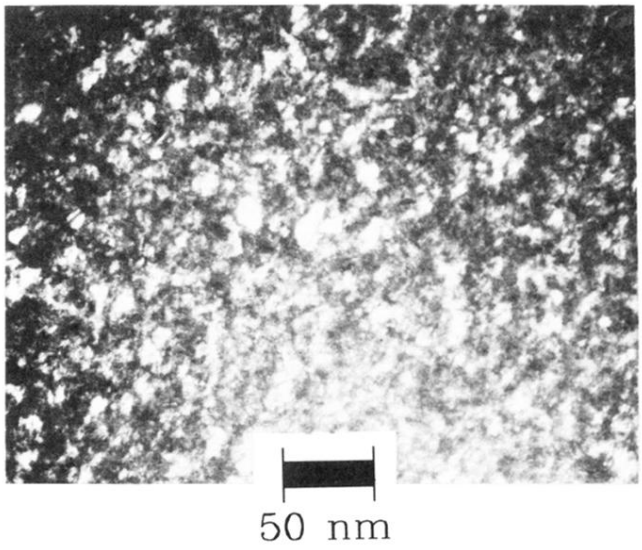

FIG. 1. Dark-field TEM plan-view micrograph of a SIPOS sample containing 15 at. % O. A fine-grain polycrystalline structure is evidenced by the micrograph.